ARTICLES

Dynamical Solvent Control of Electron Transfer in a Flexible, Tethered Donor−Acceptor Pair

Na'il Saleh† and John F. Kauffman*

Department of Chemistry, University of Missouri−Columbia, Columbia, Missouri 65211-7600

Received: April 20, 2004; In Final Form: June 30, 2004

The solvent dependence of the photoinduced intramolecular charge transfer rate constants of 1-(9-anthryl)-3-(4-dimethylaniline)propane (ADMA) is investigated by picosecond time-resolved fluorescence spectroscopy in polar solvents. ADMA undergoes electron transfer by two distinct mechanisms, depending on the solvent polarity. In nonpolar solvents the excited ADMA molecule must fold prior to electron transfer, whereas in polar solvents electron transfer can occur in an extended conformation. In polar solvents, ADMA exhibits biexponential fluorescence decay. This is consistent with the proposed polar mechanism of electron transfer, in which electron transfer occurs in an extended conformation, and is followed by conformational interconversion to an emissive, folded conformation. Examination of the kinetic expressions for the time-dependent population of the locally excited state of ADMA indicates that the fast decay time of the fluorescence decay is approximately equal to the inverse of the forward electron-transfer rate constant. A linear correlation is observed between the fast decay time and the amplitude weighted average solvation time determined from time-dependent Stokes shift measurements. This indicates that solvent dynamics influences the electron-transfer rate. Analysis of the results on the basis of an expression for the rate constant of adiabatic electron transfer demonstrates that the results are consistent with previous estimates of the reorganization energy and electron-transfer barrier using a dielectric continuum model. Comparison of ADMA electron-transfer rate constants in ethers with electron-transfer rate constants in polar solvents shows that ADMA undergoes electron transfer by a mechanism that is intermediate between the polar and nonpolar mechanisms in solvents of intermediate polarity.

I. Introduction

Zusman derived an expression that predicts an inverse dependence of the electron-transfer rate constant on the solvent longitudinal relaxation time in 1980.[1] Since then, a formidable volume of theoretical work on dynamic solvent effects on electron transfer has been published.[2−10] It is now reasonably well established[11] that in the classical limit, the rate constant for electron transfer in dissipative environments can be approximately described by expressions of the form,[8]

$$k_f = \frac{V^2}{1 + \frac{2\pi V^2}{\lambda \hbar \omega_c}} \sqrt{\frac{\pi}{\hbar^2 \lambda kT}} \exp\left(\frac{-\Delta G^\dagger}{kT}\right) \qquad (1)$$

where k_f is the forward electron-transfer rate constant, V is the coupling matrix element between the zeroth order electronic states, λ is the reorganization energy, $\hbar$ is Planck's constant over 2π, kT is the thermal energy, $\Delta G^\dagger$ is the activation barrier given by the Marcus expression, and ω_c is a frequency that characterizes the spectral density of the dissipative solvent bath (e.g., the peak frequency). In these expressions the "adiabaticity parameter" is defined as $g = 2\pi V^2/\lambda\hbar\omega_c$. When $g \ll 1$, the electron-transfer rate constant is proportional to V^2, and the solvent frequency parameter has an insignificant effect on the preexponential factor. These are characteristics of the nonadiabatic limit, and they are expected to occur when ω_c is large relative to the tunneling frequency, $2V/\hbar$. When ω_c is small compared to the tunneling frequency, passage over the barrier is primarily determined by the dissipative dynamics. In this "adiabatic" regime, $g \gg 1$, and the electron-transfer rate constant simplifies to

$$k_f = \omega_c \sqrt{\frac{\lambda}{4\pi kT}} \exp\left(\frac{-\Delta G^\dagger}{kT}\right) \qquad (2)$$

Though some studies of solvent effects on electron-transfer rates have shown that electron-transfer rate constants are inversely proportional to the solvent longitudinal relaxation time, τ_l,[12] Barbara and co-workers demonstrated that this is not a general phenomenon.[13] Furthermore, they demonstrated that solvent-dependent electron-transfer rate constants of bianthryl were well correlated with time constants of time-dependent Stokes shifts (TDSS) of coumarin chromophores.[14−16] Their results suggested that relaxation times measured by the TDSS method reflect solvent properties, and are independent of the chromophore. Over the past 15 years, TDSS measurements of fluorescent molecules have been examined extensively.[17−46]

* To whom correspondence should be addressed. E-mail: kauffmanj@missouri.edu.

† Current address: Chemistry Department, Yarmouk University, 21163 Irbid, Jordan.

10.1021/jp048279j CCC: $27.50
Published on Web 08/11/2004

Maroncelli et al.[25] have developed an approximate expression that predicts a power law relationship between the collective solvation correlation function measured by TDSS and the dipole correlation function of a single solvent molecule. The temporal response of a solvent to a change in solute charge distribution has been shown to exhibit behavior that can be anticipated on the basis of dielectric dispersion measurements with one caveat: the dielectric function must be measured into the terahertz regime.[47] The remarkable agreement between solvent response functions determined by TDSS and solvent response functions calculated from broad spectrum dielectric functions indicates that the power law relationship between the solvation correlation function and the single molecule solvent dipole correlation function also holds between the solvation correlation function and the longitudinal component of the collective dipole correlation function that characterizes the dielectric dispersion data. Maroncelli[25] interprets the power law exponent as characteristic of the degree of collectivity in the solvent motion with respect to the particular measurement that is used to observe solvent dynamics.[47] As solvent polarity increases, the exponent increases, and the magnitude of rotational motion required to achieve an equilibrium solvent configuration diminishes. As a result, the low amplitude solvent inertial response in highly polar solvents such as water and acetonitrile accounts for more than 50% of the measured Stokes shift of coumarins,[48] which explains why terahertz dielectric dispersion data are required to achieve agreement between TDSS and dielectric spectroscopy. Importantly, these studies indicate that the response of solvent in TDSS measurements is independent of the solute to a first approximation. This is especially relevant to studies of dynamic solvent control of electron-transfer kinetics.

Over the past decade, the time resolution of TDSS measurements has improved, due to recent developments in ultrafast laser technology. Parameters of multiexponential TDSS temporal profiles for several chromophores have been tabulated for dozens of solvents, and at this point in time a significant database of dynamic solvation data based on these measurements is available.[17] In light of these developments, it is surprising that relatively few time-dependent studies of dynamical solvent control of electron-transfer rate constants that utilize this information have been reported. Horng et al.[49] reported excited-state electron-transfer rate constants for 9-(4-biphenyl)-10-methylacridinium·PF_6 in a variety of solvents, and compared them with the average solvation time of Coumarin 153 in these solvents. In polar solvents they observed a linear correlation between the inverse of the electron-transfer rate constant and the average solvation time. Kubiak and co-workers[50−52] have presented spectroscopic evidence for dynamical solvent control of electron transfer between two mixed valence trinuclear ruthenium clusters connected by a bridging ligand. The molecule is symmetric except for the cluster oxidation states, which differ by one electron. Infrared bands of single carbonyl ligands attached to each cluster exhibit slightly different shifts, reflecting the difference in cluster oxidation states. Electron transfer between clusters causes the bands to coalesce, and the IR band shape can be used to estimate the time scale of electron transfer. The electronic coupling constants estimated from intervalence charge-transfer spectra are in the range of 1000−2000 cm^{-1}, indicating that the reaction is strongly adiabatic. Londergan et al.[51] report that solvent-dependent variations in the infrared band shape of this compound reflect a correlation between the time scale of electron transfer and the average solvent relaxation times of polar solvents that have been tabulated by Horng et al.[17] Solvent dynamics have also been implicated in ultrafast charge-transfer-to-solvent that results from photodetachment of atomic anions in solution,[53,54] but the solvation rate is primarily sensitive to translational dynamics owing to the considerable change in solute size that accompanies these reactions, and does not appear to be strongly correlated with solvent dynamics measure via the TDSS method.

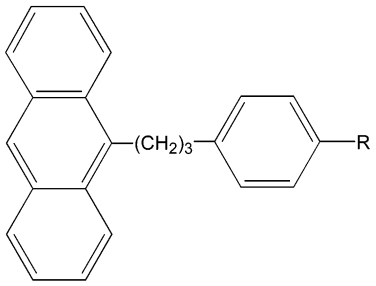

Figure 1. Structure of ADMA (R = $N(CH_3)_2$) and APP (R = H). See Figure 2 for representative structures.

The purpose of this paper is to present evidence for dynamical solvent control of photoinitiated electron transfer in a flexible, tethered donor acceptor pair, 1-(9-anthryl)-3-(4-dimethylaniline)-propane (ADMA) (see Figure 1). The anthracene moiety of ADMA can be selectively excited with 387-nm light. The subsequent emission spectrum exhibits anthracene-like emission in the 390−480-nm region, as well as a Gaussian charge-transfer band whose peak wavelength depends on the Lippert−Mataga polarity function of the solvent.[55] Mataga and co-workers[56] demonstrated that the emission arises from the folded conformation of the ADMA charge transfer state. We have investigated the temporally and spectrally resolved fluorescence of this molecule in numerous pure solvents and mixed solvent systems.[55,57−60] In this paper we examine the temporal decay of the anthracene-like emission of ADMA dissolved in solvents with dielectric constants greater than 5, in which electron transfer is expected to occur in the extended conformation of ADMA.

II. Experimental Section

ADMA and APP (1-(9-anthryl)-3-phenylpropane), Figure 1, were synthesized according to the method outlined previously.[55,57] The solvents were obtained in the purest commercially available form, degassed with argon, and used without further purification. All measurements were made on 10^{-5} M samples thermostated at 25 °C. Fluorescence decays were measured with the time-correlated photon counting (TCPC) method, using a dye laser pumped by a frequency doubled, mode-locked, diode pumped Nd:YAG laser. The dye laser was cavity dumped at 4 MHz. A (BBO) crystal combined a 1064-nm IR beam with a 608-nm beam from the dye laser in order to obtain a 387-nm beam for excitation. The excitation beam was vertically polarized and the emission was collected at the magic angle. The time-resolved emission wavelength was selected with a 420-nm band-pass filter (10-nm fwhm), and was collected by a microchannel plate PMT (Hamamatsu, R 3809U-50). A typical instrument function has a 70-ps fwhm. The data were analyzed by the iterative reconvolution method, using software of our own design that utilizes the Marquardt−Levenberg algorithm to minimize χ^2, resulting in a time resolution of ∼12 ps. Fluorescence spectra were recorded with a photon counting fluorimeter of our own design.[61]

III. Kinetic Analysis and Emission from the Locally Excited State

The mechanism of photoinitiated electron transfer in ADMA was elucidated by Eisenthal and co-workers[62−65] and Mataga

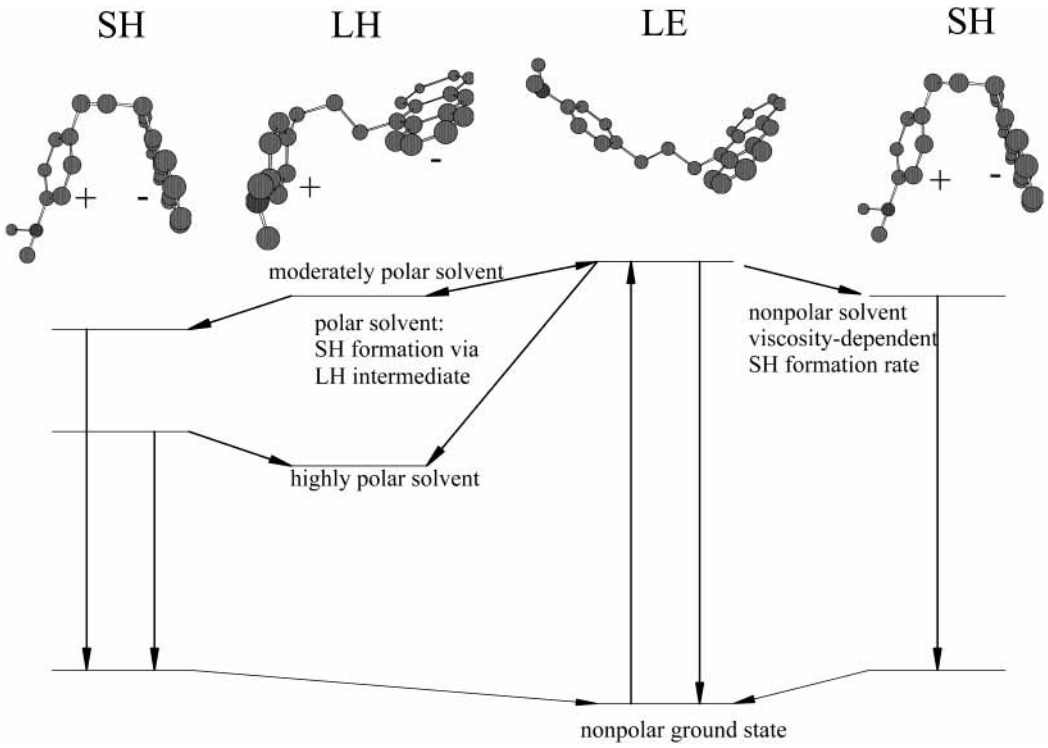

Figure 2. Energy level scheme that governs excited state isomerization kinetics of ADMA. The scheme demonstrates that sandwich heteroexcimer (SH) state formation is mediated by both solvent viscosity and solvent polarity. In polar solvents the favored pathway to the SH state is through the charge-separated loose heteroexcimer (LH) intermediate. The nonemissive LH state becomes the low energy configuration in highly polar solvents.

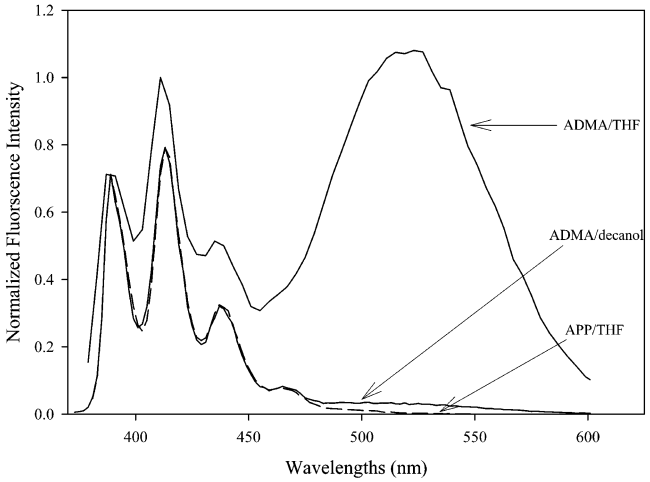

Figure 3. Fluorescence spectra of ADMA in tetrahydrofuran and decanol, and of APP in tetrahydrofuran. The spectra are normalized at the 390-nm peak. ADMA in THF exhibits a much larger charge transfer band intensity, because the electron-transfer reaction is much faster in THF than in decanol, resulting in a larger quantum yield for charge transfer emission in THF. APP in THF and ADMA in decanol are nearly identical in the region associated with emission from the anthracene locally excited state, as expected.

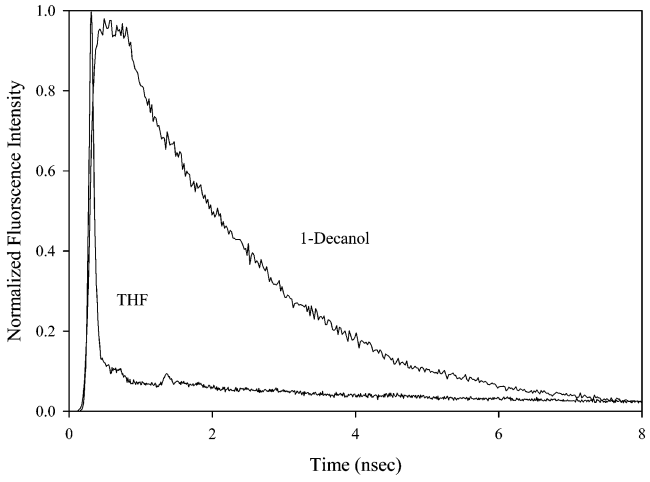

Figure 4. Fluorescence decays of ADMA in tetrahydrofuran and decanol.

and co-workers[56,66−69] two decades ago. Their mechanism is summarized in Figure 2. Following selective excitation of the locally excited (LE) anthracene moiety, the dimethylaniline moiety donates an electron to the excited anthracene moiety, and the mechanism of electron transfer depends on the solvent dielectric constant. In nonpolar solvents, the molecule must fold into a sandwich geometry prior to electron transfer. Mataga[56] referred to the resulting folded exciplex as the "sandwich heteroexcimer" (SH) state of the molecule. The fluorescence decay of the anthracene-like emission exhibits a viscosity-dependent single-exponential decay profile in nonpolar solvents,[65] indicating that the forward electron transfer is preceded by folding, and the back-electron transfer is highly unfavorable.

In polar solvents, charge transfer can occur when ADMA is in an extended conformation, resulting in a "loose heteroexcimer" (LH).[56] Following electron transfer in the extended conformation, ADMA undergoes intramolecular conformational rearrangement to the emissive SH state if the dielectric constant of the solvent is less than ∼20. When the solvent is sufficiently polar ($\epsilon > 20$), the extended charge transfer conformation is stable, and no CT emission is observed, because the loose heteroexcimer is nonemissive.[70] While several prior papers have demonstrated the dependence of the ADMA reaction pathway on the solvent dielectric constant,[69,71,72] Figures 3 and 4 highlight the inadequacy of this parameter with respect to the charge

TABLE 1: Decay Parameters for ADMA in Various Solvents

solvents	ϵ_0	n	CT peak shift (nm)	A_f	τ_f (ns)	A_s	τ_s (ns)	A_s/A_f	η (cP)	$10^{-8}k_\eta$ (s^{-1})	τ_{app} (ns)
hexane	1.89	1.38	474.60	1.00	1.73				0.30	3.62	4.29
cyclohexane	2.02	1.43	473.20	1.00	2.48				0.91	2.09	5.85
hexadecane	2.05	1.43	471.80	1.00	3.40				3.04	1.15	6.05
mineral oil	2.05	1.47	476.70	1.00	5.90				23.10	0.42	7.80
dibutyl ether	3.08	1.40	492.30	1.00	2.16				0.65	2.47	6.39
dipropyl ether	3.38	1.38	496.00	1.00	1.32				0.40	3.12	4.36
diethyl ether	4.26	1.35	504.20	1.00	0.39				0.22	4.16	4.10
tert-amylOH	5.82	1.41	514.60	0.99	0.71	0.01	3.73	0.01	3.48	1.07	6.58
EtOAc	6.02	1.37	522.60	0.995	0.02	0.01	4.68	0.01	0.42	3.04	7.02
BuCl	7.39	1.40	509.00	0.95	0.29	0.05	3.34	0.05	0.42	3.04	7.24
THF	7.58	1.41	523.90	0.99	0.017	0.01	6.50	0.01	0.70	2.37	8.87
decanol	8.03	1.44	520.00	0.98	1.84	0.02	4.07	0.02	10.90	0.61	7.87
CH_2Cl_2	9.08	1.42	526.10	0.994	0.009	0.006	6.74	0.006	0.41	3.09	7.85
octanol	9.86	1.43	526.00	0.90	1.13	0.10	6.83	0.11	7.15	0.75	7.35
propanol	20.43	1.38	534.00	0.996	0.12	0.004	4.30	0.00	1.95	1.43	7.23
EtOH	24.32	1.36	537.10	0.99	0.06	0.01	4.48	0.01	1.27	1.76	5.18
propylene glycol	32.00	1.43	537.00	0.85	0.05	0.02	8.56	0.02	40.40	0.32	9.74

SCHEME 1

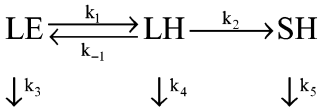

transfer rate. Figure 3 shows the spectra of ADMA dissolved in THF and *n*-decanol, two solvents with very similar dielectric constants, but widely varying solvent relaxation times. The spectrum of APP in THF is also shown. Figure 4 shows the fluorescence decays of ADMA in THF and decanol. The reactant concentration decays much more rapidly in THF than in decanol, and this has consequences for the emission spectra shown inFigure 3b. A significantly larger fraction of excited ADMA molecules decay via the CT state when the solute is dissolved in THF in comparison with decanol, because the CT reaction occurs within a few tens of picoseconds following excitation.

Equation 2 predicts that the electron-transfer rate constant (k_1 in Scheme 1) depends on the solvent relaxation time, and in the following paragraphs we demonstrate that k_1 can be easily extracted from the fluorescence decay of the LE state of ADMA. Scheme 1 summarizes the polar kinetic mechanism appropriate for the present analysis.

The expression for the time-dependent population of the LE state following impulsive excitation is[69,73]

$$[\mathrm{LE}] = A_f e^{-\lambda_f t} + A_s e^{-\lambda_s t} \tag{3}$$

$$\lambda_f = {}^1/_2\{(k_1 + k_3 + k_{-1} + k_2 + k_4) + \sqrt{(k_1 + k_3 - k_{-1} - k_2 - k_4)^2 + 4k_1k_{-1}}\}$$

$$\lambda_s = {}^1/_2\{(k_1 + k_3 + k_{-1} + k_2 + k_4) - \sqrt{(k_1 + k_3 - k_{-1} - k_2 - k_4)^2 + 4k_1k_{-1}}\} \tag{4}$$

and

$$A_f = \frac{k_1 + k_3 - \lambda_s}{\lambda_f - \lambda_s}[\mathrm{LE}_0]$$

$$A_s = \frac{\lambda_f - k_1 - k_3}{\lambda_f - \lambda_s}[\mathrm{LE}_0] \tag{5}$$

The time constants for the fast and slow components of the decay are $\tau_f = 1/\lambda_f$ and $\tau_s = 1/\lambda_s$, respectively. The LE state population decays according to a biexponential rate law when the polar mechanism is operative, and a single-exponential decay when the nonpolar mechanism is operative. This provides a convenient method to characterize solvents as polar or nonpolar with respect to ADMA charge transfer. Decay parameters for several solvents are given in Table 1. Studies of ADMA charge transfer in neat and mixed liquids show that solvents with dielectric constants below 5 support the nonpolar pathway, and solvents with dielectric constants above 5 support the polar pathway.[59] This is evident in Table 1. The emission maximum of the SH emission band is also listed in the table, and it is evident that the peak shift depends on the solvent dielectric constant.

In general the time constants and amplitudes given by eq 3 cannot be easily interpreted with respect to specific elementary processes in Scheme 1. However, previous investigations of ADMA kinetics have resulted in accurate estimates of several of the rate constants, and these lead us to conclude that the λ_f is equal to the forward electron-transfer rate, k_1. The considerations that lead to this conclusion are briefly described here. k_3 can be determined experimentally by measuring the fluorescence decay rate of APP, a model compound whose radiative and nonradiative decay rates are expected to mimic the rates of ADMA,[74] except that APP cannot undergo electron transfer. Thus $k_3 = (\tau_{APP})^{-1}$. Solvent-dependent fluorescence lifetimes of APP are reported in Table 1. Mataga and co-workers[69] observed the transient absorbance spectrum of the anthracene radical anion of ADMA in polar solvents after photoexcitation at time delays as long as 2.5 ns. We therefore estimate the value of $k_4 \sim 10^8$ s^{-1}. k_5 is also found to be $\sim 10^7$ s^{-1} from the fluorescence lifetime of the SH emission. k_2 characterizes the rate of formation of the SH conformation from the LH conformation via intramolecular folding. We anticipate that this folding reaction will depend on viscosity on the basis of the observed viscosity power law dependence of the charge-transfer rate in nonpolar solvents.[65,72] The viscosity power law offers a convenient means of estimating k_2, but two phenomena must be considered to do so. First, it must be recognized that ADMA may undergo several folding−unfolding cycles before electron transfer occurs in nonpolar solvents,[72] and therefore the viscosity power law only provides a lower limit on the folding rate constant. Estimates of the activation barriers to unfolding and charge transfer in nonpolar solvents suggest that the folding rate may be as much as a factor of 3 larger than the charge-transfer rate determined from the viscosity power law.[72] Second, in the polar mechanism, the charged LH state will also

TABLE 2: Solvent Relaxation Parameters from TDSS Measurements

solvents[a]	ϵ	a_1	τ_1 (ps)	a_2	τ_2 (ps)	a_3	τ_3 (ps)	a_4	τ_4 (ps)	τ_0 (ps)	τ_{avg} (ps)	$\tau_{(1/e)}$ (ps)	τ_f (ps)
CH_2Cl_2	9.08	0.52	0.14	0.48	1.02					0.25	0.57	0.38	9
THF	7.58	0.45	0.23	0.55	1.52					0.43	0.94	0.70	17
EtOAc[b]	6.02	1.00	2.70							2.70	2.70	2.69	21
EtOH	24.32	0.09	0.03	0.23	0.39	0.18	5.03	0.50	29.6	0.29	15.9	10.9	60
propanol	20.43	0.09	0.03	0.17	0.34	0.23	6.57	0.52	47.8	0.29	26.2	18.0	119
decanol	8.03	0.12	0.03	0.06	0.58	0.18	43.3	0.64	373.0	0.24	244.7	205.0	1840
octanol[c]	9.86	0.20	45.0	0.80	300.0					140.6	249.0	233.2	1130
dibutyl ether[b]	3.08	1.00	12.00							12.00	12.00	12.00	2158
diethyl ether[b]	4.26	0.71	1.20	0.29	3.00					1.45	1.72	0.79	385

[a] Solvation data is taken from ref 17 unless noted otherwise. The authors report a 125 fs instrument response function. [b] Ethyl acetate and ether data are taken from ref 33. The authors report a 300 fs instrument response function. [c] Octanol solvation data are taken from ref 75. The authors report a 50 ps instrument response function.

experience dielectric friction that will reduce the value of k_2. These two phenomena have opposing effects on the difference between the folding rate and the charge-transfer rate determined from the viscosity power law. Thus the viscosity power law,[72]

$$\frac{1}{k_\eta} = 5.03\eta^{0.50} \tag{6}$$

may provide a reasonable approximation for k_2. Values of k_η based on eq 6 are tabulated in Table 1, with typical values in the range of 10^8 s^{-1}.

k_1 and k_{-1} are unknown, but the introductory discussion suggests that k_1, the forward electron-transfer rate, will depend on the solvent relaxation time. k_{-1} is expected to have an upper limit equal to k_1, and a lower limit of zero. Clearly, there is uncertainty in the values of k_2 and k_4, and we have examined the sensitivity of the time constants and amplitudes in eq 3 to variations in these parameters. We have found that when $k_4 \leq 7 \times 10^8$ s^{-1} and $k_\eta \leq k_2 \leq 3k_\eta$, then to a very good approximation, $\lambda_f = k_1 + k_{-1} + k_3$. Thus if k_1 is significantly larger than k_{-1} and k_3, then the fast decay time in the fluorescence decay of the ADMA LE state is equal to the inverse of the forward charge-transfer rate constant. Furthermore, when $k_1 \geq 10^{10}$ s^{-1}, then the following equality holds.

$$\frac{A_s}{A_f} = \frac{k_{-1}}{k_1} \tag{7}$$

Equation 7 allows us to estimate k_{-1} from the ratio of experimental magnitudes of the slow and fast decay components. A_s/A_f is tabulated in Table 1, and indicates that back electron transfer is at least an order of magnitude slower and typically 2 orders of magnitude slower than forward electron transfer in polar solvents. Thus we find that $\lambda_f \approx k_1$ as long as $k_1 \geq 10^9$ s^{-1}, since $k_3 \approx 10^8$ s^{-1}. Table 1 indicates that $1/\tau_f$ is greater than 10^9 s^{-1} for most of these solvents. Viscous solvents with low dielectric constants exhibit slightly lower rate constants for forward electron transfer, as one might expect on the basis of eq 2. This discussion parametrizes the conditions under which the short time constant of the biexponential fluorescence decay of ADMA in polar solvents can be viewed as the forward electron-transfer time, and indicates that this is a good approximation for the solvents considered in Table 2.

IV. Results and Discussion

Table 2 presents the TDSS-based solvent relaxation parameters from refs 17, 33, and 75 for several of the solvents used in this study, along with characteristic decay times for solvent relaxation that have been discussed by Horng et al.[17] The characteristic decay times are defined as follows. τ_0 is the inverse of the initial solvation rate, which characterizes the inertial contribution, and is calculated as $\tau_0^{-1} = \sum_i a_i\tau_i^{-1}$. τ_{avg} is the amplitude weighted average of the solvation times, calculated as $\tau_{avg} = \sum_i a_i\tau_i$. $\tau_{1/e}$ is the time required for the solvation correlation function to reach a value of 0.368. The fast decay constant, τ_f, of ADMA from Table 1 has also been reproduced in Table 2.

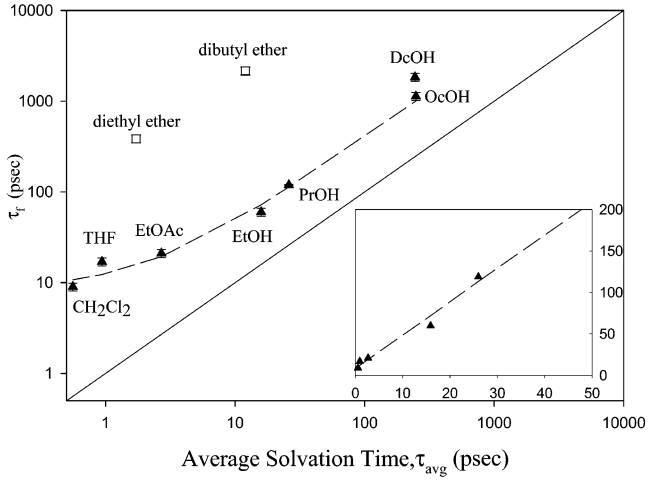

Figure 5. Fast time constant of the measured fluorescence decay, τ_f, versus the amplitude weighted average solvation time, τ_{avg}, from TDSS measurements. τ_{avg} are taken from refs 17, 33, and 75, as described in Table 2. The solid line is a guide to the eye to indicate where $\tau_f = \tau_{avg}$. The dashed line is the linear regression of the polar solvent data, which is indicated by solid triangles. The inset shows the correlation on a linear scale, along with the regression line. Open squares are ethers, whose polarity is intermediate between nonpolar and polar solvents with respect to ADMA electron transfer.

Figure 5 is a plot of the measured value of τ_f versus τ_{avg} for seven polar solvents with dielectric constants greater than 5. Two additional data points are also shown for dibutyl ether and diethyl ether whose dielectric constants are 3.1 and 4.3, respectively, and the significance of these data points will be discussed below. The plot includes a line with slope = 1 and intercept = 0 as a guide to the eye. The measured values of the forward electron-transfer times are slower than the average solvation time, but a linear correlation is evident. A similar correlation exists between τ_f and $\tau_{1/e}$. However, a linear correlation is not evident between τ_f and τ_0, nor between τ_f and the solvent dielectric constant. The octanol data point is expected to be artificially high on this plot along the *x*-axis, because the time resolution of the instrument used to measure the TDSS decay was 50 ps,[75] and therefore was not able to resolve the short time decays that can be anticipated on the basis of femtosecond measurements of other alcohols.[17] The THF and CH_2Cl_2 data points may also be artificially high along the *y*-axis,

TABLE 3: Calculated Potential Energy Parameters for the Extended Charge Transfer Reaction of ADMA

solvents	ϵ	n	λ (kJ/mol)	ΔG_{ct}^{ϵ} (kJ/mol)	$\Delta G^{\dagger}$ (kJ/mol)
CH_2Cl_2	9.08	1.42	114	−22.0	18.6
THF	7.58	1.41	112	−17.5	20.0
EtOAc	6.02	1.37	111	−10.8	22.5
EtOH	24.32	1.36	137	−35.5	18.8
propanol	20.43	1.38	132	−34.0	18.1
decanol	8.03	1.44	109	−19.0	18.6
octanol	9.86	1.43	115	−23.6	18.1

because the reported values of τ_f are a factor of 2 faster than the estimated time resolution limit of our TCPC instrument. Sensitivity analysis demonstrates that these considerations will have a small effect (~3% change in *y*-intercept, 1% change in slope) on a linear regression analysis of the results.

We will now estimate values of the parameters in eq 1 for ADMA charge transfer in polar solvents. In a recent paper,[72] we calculated solvent-dependent values of λ and ΔG_{ct}^{ϵ}, the free energy of electron transfer, for the ADMA charge-transfer reaction in the folded conformation as a function of solvent dielectric constant using continuum models. The values for $\Delta G^{\dagger}$ were determined from the Marcus equation,[76]

$$\Delta G^{\dagger} = \frac{\lambda_0^{\epsilon}}{4}\left(1 + \frac{\Delta G_{ct}^{\epsilon}}{\lambda_0^{\epsilon}}\right)^2 \tag{8}$$

where $\lambda_0^{\epsilon} = \lambda_v + \lambda_s^{\epsilon}$ is the sum of the inner sphere (λ_v) and solvent (λ_s^{ϵ}) contributions to the reorganization energy. ΔG_{ct}^{ϵ} was determined using the Rehm−Weller expression, corrected for solvent-dependent ion solvation energies, distance-dependent Coulomb energies, and the steric energy of the folded conformation. ΔG_{ct}^{ϵ} for the extended conformation was also calculated in the previous paper,[72] and the results offered a thermodynamic basis for the observed dependence of the charge-transfer mechanism on solvent dielectric constant. Charge transfer is exothermic in the folded conformation for all values of the solvent dielectric constant, including the vacuum environment. On the other hand, charge transfer in the extended conformation is endothermic below a solvent dielectric constant of 5, and exothermic for dielectric constants greater than 5. Calculated values of ΔG_{ct}^{ϵ} for the extended conformation at dielectric constants associated with the polar solvents used in Figure 5 have been tabulated in Table 3. We have estimated solvent and distance dependent values for λ_s^{ϵ} using the dielectric continuum Marcus model,[76,77]

$$\lambda_s^{\epsilon}(r_{A-D}) = \frac{\Delta q^2}{4\pi\epsilon_0}\left(\frac{1}{n^2} - \frac{1}{\epsilon}\right)\left(\frac{1}{2a_D} + \frac{1}{2a_A} - \frac{1}{r_{A-D}}\right) \tag{9}$$

where q is the charge transferred (assumed to be 1 electron in this system), n and ϵ are the solvent refractive index and dielectric constant, respectively, a_D and a_A are the donor and acceptor cavity radii (3.5 and 4 Å, respectively, based on solvent excluded volumes around ab initio structures of the donor and acceptor ions, see ref 72 for details), and r_{A-D} is the separation distance between reactants (8 Å, see ref 72) at the time of electron transfer. Ando[77] has shown that eq 9 produces the same trend with respect to distance as potential energy surfaces based on simulation of the bimolecular electron-transfer reaction of anthracene and dimethylaniline. In a recent publication, we estimated λ_v to be 38 kJ/mol, and for the present analysis we will assume that the inner sphere reorganization energy is independent of the distance between the reactants. Values of the total reorganization energy along with values for $\Delta G^{\dagger}$ calculated via eq 8 are tabulated in Table 3.

In principle, eq 1 can be used to estimate V, but direct application of eq 1 is not expected to be reliable in the present case, owing to the small number of degrees of freedom in the fitting process. Equation 1 can be rewritten to emphasize the linear relationship between the fast fluorescence lifetime and the characteristic solvation time,

$$\tau_f = \left[\sqrt{\frac{kT}{\pi\lambda}}\,\tau_{avg} + \sqrt{\frac{\hbar^2\lambda kT}{\pi V^4}}\right]\exp\left(\frac{\Delta G^{\dagger}}{kT}\right) \tag{10}$$

If λ and $\Delta G^{\dagger}$ are constant, then the parameters of a linear regression analysis of τ_f against τ_{avg} can be used to determine V according to the expression,

$$V = \hbar\lambda\sqrt{\frac{m}{b}} \tag{11}$$

where m is the slope of the regression line, and b is the intercept. Though variation in the values of λ and $\Delta G^{\dagger}$ is evident in Table 3, it is instructive to perform this calculation with the average value of λ (119 ± 11 kJ/mol). The dashed line in Figure 5 represents the linear regression of τ_f versus τ_{avg}, with $b = 8.5 \pm 5$ ps and $m = 4 \pm 0.4$ ($R^2 = 0.98$).[78] Using these regression parameters, eq 11 gives $V = 160 \pm 67$ cm^{-1}. (The uncertainty is the standard deviation of V determined via conventional differential rules for propagation of error neglecting covariance, and is dominated by the intercept parameter variance.) V is expected to depend on distance, and Ando's simulations of the bimolecular charge-transfer reaction from dimethylaniline to excited-state anthracene confirm this expectation.[77] Ando's empirical correlation between V (in cm^{-1}) and r_{A-D} (in Å) is given by

$$|V(r_{A-D})|^2 = |671\ \text{cm}^{-1}|^2 \exp[-0.83(r_{A-D} - 5)] \tag{12}$$

and predicts 190-cm^{-1} coupling at 8 Å in acetonitrile. Thus our estimate based on the linear correlation observed in Figure 5 agrees with Ando's estimate of V, though there is some uncertainty in these estimates. Equation 12 indicates that the coupling strength doubles at a distance of 6.4 Å, whereas the activation barrier and reorganization energy are expected to decrease with decreasing distance. But while small solute conformational fluctuations are expected to modulate the electron-transfer reaction rate, it is apparent from Figure 5 that the preexponential factor in eq 1 is dominated by the solvent relaxation time for polar solvents. These results indicate that solvent dynamics has a significant influence on the rate of electron transfer from dimethylaniline to excited anthracene in the tethered ADMA molecule. Apparently the average solvation time, τ_{avg}, provides an adequate characterization of the spectral density of the dissipative bath with respect to electron transfer in ADMA. Ando's simulation of the bimolecular excited-state electron-transfer reaction between anthracene and dimethylaniline shows that the reaction is adiabatic on the basis of the strength of the electronic state coupling, which increases to ~700 cm^{-1} at $r_{A-D} \approx 5$ Å.[77] This is consistent with our experimental results, which indicate that excited-state electron transfer in the extended conformation of the tethered ADMA molecule is an adiabatic process in polar solvents with respect to the assumptions used to derive eq 2.

The ethers have been included in Figure 5 because they represent solvents that bridge the polar and nonpolar regimes. In a previous publication, we demonstrated that the electron-

transfer reaction of ADMA is accelerated in these solvents, beyond the acceleration expected on the basis of product stabilization as predicted by Marcus theory. We postulated that in this regime, the donor−acceptor distance at which electron transfer occurs in dibutyl ether and diethyl ether is between r_{A-D} in the folded and extended conformations. This postulate implies that if electron transfer is possible in a partially folded conformation but not in the extended conformation, then it will occur faster than expectation based on the nonpolar mechanism, but slower than expectation based on the polar mechanism. The ethers exhibit single exponential fluorescence decays, and we have plotted their fluorescence lifetimes along the *y*-axis of Figure 4 versus their average solvation times as determined by the TDSS method. It is clear from this plot that the electron-transfer rate for ethers is considerably slower than that expected on the basis of their solvation dynamics. This is consistent with the postulate that ADMA in these solvents undergoes electron transfer by a mechanism that is intermediate between the polar and nonpolar mechanisms, and therefore they reflect electron-transfer rates in the transition regime.

We have demonstrated that electron transfer of a tethered donor−acceptor pair is controlled by solvent relaxation in polar solvents. Solvent motion induces electron transfer, and also stabilizes the charge-separated form of the molecule on the time scale of solvent relaxation. The bimolecular electron-transfer reaction between a dimethylaniline donor and an excited anthracene acceptor has also been thoroughly investigated.[79−81] The absorption and emission spectra of the tethered system are nearly identical with those of the bimolecular system, but the rate of electron transfer in the bimolecular system is diffusion limited. This prevents observation of dynamic solvent effects in the bimolecular anthracene−dimethylaniline system, as well as numerous other bimolecular systems that undergo electron transfer by the same mechanism. However, the results of the present work indicate that dynamic solvent effects play an important role in the bimolecular systems, even though the effects cannot be measured in dilute solution.

Acknowledgment. This work was supported in part by the National Science Foundation, and by the University of Missouri Department of Chemistry. N.S. would like to acknowledge the support of Yarmouk University through fellowship grant no. PER/12/3929 dated August 9, 1998.

References and Notes

(1) Zusman, L. D. *Chem. Phys.* **1980**, *49*, 295.

(2) The following references only enumerate a few of the early papers in this area, and a few recent articles. For a recent review of electron-transfer theory, see ref 3.

(3) Jortner, J.; Bixon, M. *Electron Transfer−From Isolated Molecules to Biomolecules*; Wiley: New York, 1999; Vols. 106/107.

(4) Ankerhold, J.; Lehle, H. *J. Chem. Phys.* **2004**, *120*, 1436.

(5) Zhang, M.-L.; Zhang, S.; Pollak, E. *J. Chem. Phys.* **2003**, *119*, 11864.

(6) Casado-Pascual, J.; Morillo, M.; Goychuk, I.; Hanggi, P. *J. Chem. Phys.* **2003**, *118*, 291.

(7) Frauenfelder, H.; Wolynes, P. G. *Science* **1985**, *229*, 337.

(8) Garg, A.; Onuchic, J. N.; Ambegaokar, V. *J. Chem. Phys.* **1985**, *83*, 4491.

(9) Mühlbacher, L.; Egger, R. *J. Chem. Phys.* **2003**, *118*, 179.

(10) Rips, I.; Klafter, J.; Jortner, J. *J. Phys. Chem.* **1990**, *94*, 8557.

(11) Equation 1 was taken from ref 8. Pollak and co-workers[5] have recently found that the methodology utilized in ref 8 is problematic. They derived a "generalized Zusman equation" in phase space that corrects these problems. Simulations utilizing the corrected theory are compared in ref 5 with Zusman's analytical expression, which is very similar to eq 1. The comparison demonstrates excellent agreement between theory and the analytical result in the moderate to strong damping regime. Mühlbacher and Egger have made a similar comparison in ref 9, and have prepared a "phase diagram" that parametrizes the conditions under which eq 1 is expected to hold.

(12) Kosower, E. M.; Huppert, D. *Annu. Rev. Phys. Chem.* **1986**, *37*, 127.

(13) Kahlow, M. A.; Kang, T. J.; Barbara, P. F. *J. Phys. Chem.* **1987**, *91*, 6452.

(14) Kang, T. J.; Kahlow, M. A.; Giser, D.; Swallen, S.; Nagarajan, V.; Jarzeba, W.; Barbara, P. F. *J. Phys. Chem.* **1988**, *92*, 6800.

(15) Kang, T. J.; Jarzeba, W.; Barbara, P. F.; Fonseca, T. *Chem. Phys.* **1990**, *149*, 81.

(16) Tominaga, K.; Walker, G. C.; Kang, T. J.; Barbara, P. F.; Fonseca, T. *J. Phys. Chem.* **1991**, *95*, 10485.

(17) Horng, M. L.; Gardecki, J. A.; Papazyan, A.; Maroncelli, M. *J. Phys. Chem.* **1995**, *99*, 17311.

(18) Maroncelli, M.; Fleming, G. R. *J. Chem. Phys.* **1987**, *86*, 6221.

(19) Maroncelli, M.; Fleming, G. R. *J. Chem. Phys.* **1988**, *89*, 875.

(20) Maroncelli, M.; Castner, E. W., Jr.; Bagchi, B.; Fleming, G. R. *Faraday Discuss. Chem. Soc.* **1988**, *85*, 199.

(21) Maroncelli, M.; Fleming, G. R. *J. Chem. Phys.* **1988**, *89*, 5044.

(22) Maroncelli, M.; MacInnis, J.; Fleming, G. R. *Science* (*Washington, D.C.*) **1989**, *243*, 1674.

(23) Maroncelli, M.; Fleming, G. R. *J. Chem. Phys.* **1990**, *92*, 3251.

(24) Maroncelli, M. *J. Chem. Phys.* **1991**, *94*, 2084.

(25) Maroncelli, M.; Kumar, V. P.; Papazyan, A. *J. Phys. Chem.* **1993**, *97*, 13.

(26) Maroncelli, M.; Kumar, P. V.; Papazyan, A.; Horng, M. L.; Rosenthal, S. J.; Fleming, G. R. *AIP Conf. Proc.* **1994**, *298*, 310.

(27) Kumar, P. V.; Maroncelli, M. *J. Chem. Phys.* **1995**, *103*, 3038.

(28) Castner, E. W., Jr.; Maroncelli, M.; Fleming, G. R. *J. Chem. Phys.* **1987**, *86*, 1090.

(29) Chapman, C. F.; Fee, R. S.; Maroncelli, M. *J. Phys. Chem.* **1990**, *94*, 4929.

(30) Chapman, C. F.; Maroncelli, M. *J. Phys. Chem.* **1991**, *95*, 9095.

(31) Chapman, C. F.; Fee, R. S.; Maroncelli, M. *J. Phys. Chem.* **1995**, *99*, 4811.

(32) Gardecki, J.; Horng, M. L.; Papazyan, A.; Maroncelli, M. *J. Mol. Liq.* **1995**, *65*/66.

(33) Middelhoek, E. R.; Zhang, H.; Verhoeven, J. W.; Glasbeek, M. *Chem. Phys.* **1996**, *211*, 489.

(34) Brown, R.; Middelhoek, R.; Glasbeek, M. *J. Chem. Phys.* **1999**, *111*, 3616.

(35) Reid, P. J.; Barbara, P. F. *J. Phys. Chem.* **1995**, *99*, 3554.

(36) Jarzeba, W.; Walker, G. C.; Johnson, A. E.; Barbara, P. F. *Chem. Phys.* **1991**, *152*, 57.

(37) Kahlow, M. A.; Kang, T. J.; Barbara, P. F. *J. Chem. Phys.* **1988**, *88*, 2372.

(38) Laitinen, E.; Salonen, K.; Harju, T. *J. Chem. Phys.* **1996**, *104*, 6138.

(39) Laitinen, E.; Salonen, K.; Harju, T. *J. Chem. Phys.* **1996**, *105*, 9771.

(40) Bagchi, B.; Biswas, R. *Adv. Chem. Phys.* **1999**, *109*, 207.

(41) Cichos, F.; Willert, A.; Rempel, U.; Borczyskowski, C. v. *J. Phys. Chem. A* **1997**, *101*, 8179.

(42) Goldberg, S. Y.; Bart, E.; Meltsin, A.; Fainberg, B. D.; Huppert, D. *Chem. Phys.* **1994**, *183*, 217.

(43) Gumy, J.-C.; Nicolet, O.; Vauthey, E. *J. Phys. Chem. A* **1999**, *103*, 10737.

(44) Harju, T. O.; Huizer, A. H.; Varma, C. A. G. O. *Chem. Phys.* **1995**, *200*, 215.

(45) Rosenthal, S. J.; Xie, X.; Du, M.; Fleming, G. R. *J. Chem. Phys.* **1991**, *95*, 4715.

(46) Rosenthal, S. J.; Jimenez, R.; Fleming, G. R.; Kumar, P. V.; Maroncelli, M. *J. Mol. Liq.* **1994**, *60*, 25.

(47) Castner, E. W., Jr.; Maroncelli, M. *J. Mol. Liq.* **1998**, *77*, 1.

(48) Jimenez, R.; Fleming, G. R.; Kumar, P. V.; Maroncelli, M. *Nature* **1994**, *369*, 471.

(49) Horng, M. L.; Dahl, K.; Jones, G.; Maroncelli, M. *Chem. Phys. Lett.* **1999**, *315*, 363.

(50) Londergan, C. H.; Kubiak, C. P. *Chem. Eur. J.* **2003**, *9*, 5962.

(51) Londergan, C. H.; Salsman, J. C.; Ronco, S.; Dolkas, L. M.; Kubiak, C. P. *J. Am. Chem. Soc.* **2002**, *124*, 6236.

(52) Yamaguchi, T.; Imai, N.; Ito, T.; Kubiak, C. P. *Bull. Chem. Soc. Jpn.* **2000**, *73*, 1205.

(53) Barthel, E. R.; Martini, I. B.; Keszei, E.; Schwartz, B. J. *J. Chem. Phys.* **2003**, *118*, 5916.

(54) Barthel, E. R.; Martini, I. B.; Schwartz, B. J. *J. Phys. Chem. B* **2001**, *105*, 12230.

(55) Khajehpour, M.; Kauffman, J. F. *J. Phys. Chem. A* **2000**, *104*, 7151.

(56) Migita, M.; Okada, T.; Mataga, N.; Sakata, Y.; Misumi, S.; Nakashima, N.; Yoshihara, K. *Bull. Chem. Soc. Jpn.* **1981**, *54*, 3304.

(57) Khajehpour, M.; Kauffman, J. F. *Chem. Phys. Lett.* **1998**, *297*, 141.

(58) Khajehpour, M.; Kauffman, J. F. *J. Phys. Chem. A* **2000**, *104*, 9512.

(59) Khajehpour, M.; Kauffman, J. F. *J. Phys. Chem. A* **2001**, *105*, 10316.

(60) Khajehpour, M.; Welch, C. M.; Kleiner, K. A.; Kauffman, J. F. *J. Phys. Chem. A* **2001**, *105*, 5372.
(61) Wiemers, K.; Kauffman, J. F. *J. Phys. Chem. A* **2000**, *104*, 451.
(62) Chuang, T. J.; Cox, R. J.; Eisenthal, K. B. *J. Am. Chem. Soc.* **1974**, *96*, 6828.
(63) Wang, Y.; Crawford, M. K.; Eisenthal, K. B. *J. Phys. Chem.* **1980**, *84*, 2696.
(64) Crawford, M. K.; Wang, Y.; Eisenthal, K. B. *Chem. Phys. Lett.* **1981**, *79*, 529.
(65) Wang, Y.; Crawford, M. C.; Eisenthal, K. B. *J. Am. Chem. Soc.* **1982**, *104*, 5874.
(66) Okada, T.; Fujita, T.; Kubota, M.; Masaki, S.; Mataga, N.; Ide, R.; Sakata, Y.; Misumi, S. *Chem. Phys. Lett.* **1972**, *14*, 563.
(67) Masaki, S.; Okada, T.; Mataga, N.; Sakata, Y.; Misumi, S. *Bull. Chem. Soc. Jpn.* **1976**, *44*, 1277.
(68) Migita, M.; Okada, T.; Mataga, N.; Nakashima, N.; Yoshihara, K.; Sakata, Y.; Misumi, S. *Chem. Phys. Lett.* **1980**, *72*, 229.
(69) Okada, T.; Migita, M.; Mataga, N.; Sakata, Y.; Misumi, S. *J. Am. Chem. Soc.* **1981**, *103*, 4715.
(70) In ref 69, Mataga and co-workers have suggested that the LH state emits at wavelengths longer than the SH emission. We have not observed this emission in polar solvents.
(71) Wang, Y.; Crawford, M. K.; McAuliffe, M. J.; Eisenthal, K. B. *Chem. Phys. Lett.* **1980**, *74*, 160.
(72) Kauffman, J. F.; Khajehpour, M.; Saleh, N. i. *J. Phys. Chem. A* **2004**, *108*, 3675.
(73) Matsen, F. A.; Franklin, J. L. *J. Am. Chem. Soc.* **1950**, *72*, 3337.
(74) We have tested this assumption in polar and nonpolar viscous liquids, in which the probability of electron transfer is exceedingly small, and we find that APP is indeed a good model for the ADMA fluorescence spectrum and lifetime in the absence of electron transfer.
(75) Khundkar, L. R.; Bartlett, J. T.; Biswas, M. *J. Chem. Phys.* **1995**, *102*, 6456.
(76) Marcus, R. A. *J. Chem. Phys.* **1956**, *24*, 966.
(77) Ando, K. *J. Chem. Phys.* **1994**, *101*, 2850.
(78) The assumption that the fast decay time is equal to the electron-transfer time is questionable for octanol and decanol as discussed in Section III, and therefore these data points were not utilized for the linear regression analysis.
(79) Hui, M.-H.; Ware, W. R. *J. Am. Chem. Soc.* **1976**, *98*, 4718.
(80) Basu, S. *J. Photochem.* **1979**, *11*, 9.
(81) Iwai, S.; Murata, S.; Katoh, R.; Tachiya, M.; Kikuchi, K.; Takahashi, Y. *J. Chem. Phys.* **2000**, *112*, 7111.